5-2013

Human powered Knudsen pump for pneumatic pharmaceutical delivery.

Alexander Donovan Bell
University of Louisville

HUMAN POWERED KNUDSEN PUMP FOR PNEUMATIC PHARMACEUTICAL
DELIVERY

By

Alexander Donovan Bell
B.S., University of Louisville, 2012

A Thesis
Submitted to the Faculty of the
University of Louisville
J.B. Speed School of Engineering
as Partial Fulfillment of the Requirements
for the Professional Degree

MASTER OF ENGINEERING

Department of Bioengineering

May 2013

HUMAN POWERED KNUDSEN PUMP FOR PNEUMATIC PHARMACEUTICAL DELIVERY

Submitted by:_____

Alexander Donovan Bell

A Thesis Approved On

_____

(Date)

By the Following Reading and Examination Committee:

_____

Shamus McNamara, Thesis Director

_____

Palaniappan Sethu

_____

Steven Koenig

ACKNOWLEDGEMENTS

I would like to acknowledge my thesis advisor Dr. McNamara, for his support of this project. Also, I would like to acknowledge the other members of our lab specifically A. Faiz for his help in experimentation. Finally, I would like to thank my wife for her unwavering support and without her this thesis would not exist.

ABSTRACT

Dermal wounds, including bed sores, pressure ulcers, and diabetic ulcers have a large impact on American healthcare costing up to $7 billion per year. Adequate pharmaceutical remedies applied at constant rate could prove to increase the healing rate of these wounds and save money. An infusion pump is proposed in this study to supply low flow pharmaceuticals to dermal wounds, and it is operated by a human powered Knudsen pump. This Knudsen pump provides a novel approach to the problem since it has no moving parts and it is operated by human body heat. The Knudsen pump works on the theory of thermal transpiration, which states that when a temperature difference is applied across a narrow channel, a pressure difference is formed. The temperature difference for the human powered Knudsen pump is the difference between the skin of the patient and the ambient temperature. Air flows through the Knudsen pump and applies pressure to pharmaceutical bag that drive the pharmaceuticals toward the patient. Two designs were analyzed in the study, one integrated a Knudsen pump and reservoir and the second cascaded the Knudsen pump and reservoir. The first device had a maximum output flow rate of 2.6 μL/sec and the second device had an output flow rate of 7.37 μL/hour. The study was successful in creating a human powered Knudsen pump to drive a fluid with the second design being adaptable to potentially create any flow rate necessary.

TABLE OF CONTENTS

NOMENCLATURE

ΔT = Temperature Difference

Q = Heat Flow

R = Thermal Resstance

Th = Thickness of Material

A_c = Cross Sectional Area

κ = Thermal Conductivity

C = Thermal Capacitance

m = mass

c = Specific Heat Capacity

LIST OF TABLES

LIST OF FIGURES

Chapter 1: Introduction

The device created for this master's thesis was an infusion pump utilizing a human powered Knudsen pump. An infusion pump is a device that releases a measured amount of a fluid at a specified rate [1]. These devices are very common in the medical field and can be used for a multitude of medical issues. Primarily, infusion pumps are known for their use as insulin pumps for the management of diabetes. Infusion pumps can be classified into several types based on the mechanism of delivery. Three such types include gravity, syringe, and elastomeric [2]. A gravity infusion pump holds an IV bag in the air and the force of gravity causes the pharmaceutical to evacuate the bag. The pharmaceutical is then regulated by the infusion pump. A syringe based infusion pump, on the other hand, holds the pharmaceuticals within a syringe and depresses the plunger at a specific rate and therefore flow rate. The elastomeric pump utilizes a flexible substrate; whenever pressure is applied at this location, pressure then causes the pharmaceuticals within the reservoir of the infusion pump to be driven towards the patient. The infusion pump designed in this study focuses on low flow rate usage, stemming from the discovery that low flow rates improve the healing of skin wounds, including dermal wounds [3].

Dermal wounds are classified as wounds that stretch down into the dermal layer of the skin [4, 5]. Chronic dermal wounds can arise from sources such as diabetic ulcers and bed sores. The current treatment method for these types of wounds consists of a basic wet to dry dressing applied every 4 to 6 hours. This method of treatment applies a large quantity of medication but only at every bandage replacement [6, 7]. The second leading cause of iatrogenic death in developed nations are pressure sores and they cost the United

States an estimated $7 billion per year in healthcare costs [8]. Improving upon the current treatment method of these types of sores could help to reduce the healthcare cost in America. Based on the research by Baumann, it has been shown that a constant stream of medication improves the healing process in cell culture, suggesting that it may be effective in the treatment of many types of wounds, potentially including dermal wounds and pressure sores [3]. The flow rate necessary for this medication to have a healing effect on the wound has not been determined, but a low flow rate is expected because of the cell absorption rate of the medication.

In order to create a low flow rate infusion pump, a Knudsen pump is incorporated to pneumatically drive the pharmaceuticals into the patient's wound. A Knudsen pump is ideal for this low flow rate application because it is more robust than most gas pumps. Since it does not have any moving parts, there is no wear on the device and, therefore, it could last indefinitely, as long as a temperature gradient is present. Another key aspect of this Knudsen pump is the usage of waste body heat. The Knudsen pump will be attached to the patient, who will in turn, provide the temperature gradient necessary for the device's operation. Through this process, waste body heat from a patient can be recycled as an energy source for the Knudsen pump. As long as the device is attached and the patient is producing body heat, the pump will work and supply pharmaceuticals back to the patient.

Knudsen pump theory was analyzed in order to design the most effective human powered Knudsen pump. Thermal circuit theory was also used to analyze the Knudsen pump designs. This was done to estimate the temperature difference across the Knudsen pump, which is essential in estimating the pressure generation of the pumps. Two device

designs were created and tested to prove that a human powered Knudsen pump can be created to power an infusion pump. The first design integrated a Knudsen pump and a reservoir into an all-in-one device. This device was tested by measuring the temperature necessary to cause complete evacuation of the reservoir. The second device design cascaded a Knudsen pump and a pharmaceutical reservoir. By cascading the different components of the infusion pump, they could be tested individually. The Knudsen pump of design 2 was tested by placing the device on a resistive heater emulating human skin temperature and by subsequently measuring the output air pressure and flow rate. This Knudsen pump could later be placed in series and/or in parallel to alter the pressure generation and flow rate and this was done to characterize the pump. After the characterization of the pump was performed, the needs of the reservoir were accessed. The pressure required to evacuate the reservoir was measured by measuring an applied air flow pressure and recording the corresponding distance the liquid leaving the reservoir traveled. Finally, the cascaded device was integrated and then tested. The Knudsen pump was placed on a heater set to match human skin temperature and output from the reservoir was measured.

Chapter 2: Theory

A Knudsen pump is a micro gas pump that works on the theory of thermal transpiration, which states that when a temperature gradient is applied to a narrow channel, a pressure gradient is formed [9, 10]. The flow created by thermal transpiration is known as thermal creep, which is a surface effect upon the narrow channel [11]. As air particles strike the entrance of the narrow channel they travel along the wall.

Figure 1 shows that the flux of the air particles is in the direction from the higher gas density side of the channel toward the lower density side [12]. The temperature difference affects the densities on each side of the narrow channel. Applying heat to one side of the device decreases the density at the channel interface and the opposite happens on the other side of the channel. Since the air flows from the high to low density, the air subsequently flows from the cold side to the hot side [13, 14].

Figure 2 represents the different flow profiles in the narrow channel. If the narrow channel is too wide, a reverse flow, or Poiseuille flow, is formed and negates the effect of the Knudsen pump [15, 16]. In order to prevent this from occurring, the narrow channel

Figure 1 : Illustration of the flux of air related to thermal transpiration. The equations assume the system has two closed chambers connected by a narrow channel. When a temperature difference is created by heating a cooling the chambers, a pressure difference is created in the narrow channel.

Figure 2: Illustration of flow profiles within narrow channel. Thermal creep flow is a surface effect and stays on the walls of the channel. Thermal creep flow is the flow that operates Knudsen pumps. Poiseuille flow is pressure driven flow. This flow travels from high to low pressure and works against thermal creep flow. Poiseuille flow operates in the center of a channel and if the channel is small enough this flow is negated.

must remain at a diameter near the mean free path for its environment. For instance, at atmospheric pressure the environment of ambient air has a mean free path of air diameter of 68 nm. There is also a negative correlation between the diameter of the narrow channel and the pressure obtainable by the Knudsen pump; therefore, the smaller the diameter of channel the greater the pressure obtainable [17].

The relationship between temperature and pressure can be estimated by equation 1 [18]. The variables in this equation are P_H, the pressure on the hot side of the pump, P_C, the pressure on the cold side, T_H, the temperature on the hot side, and finally T_C, which is the temperature on the cold side. The temperature side of the equation is raised to the power of n/2 where n is the number of stages of the Knudsen pump.

$$\frac{P_H}{P_C} = \left(\frac{T_H}{T_C}\right)^{\frac{n}{2}} \tag{1}$$

In order to integrate a Knudsen pump with an infusion pump it is made to be "human powered". For the human powered Knudsen pump to operate, the temperature gradient for the pump is the difference between the heat of the skin of a patient and the ambient temperature. The narrow channels for the pump are a basic filter membrane.

Filter membranes have thousands of narrow channels in parallel to one another at a specific pore size [19, 20].

Chapter 2.1: Thermal Circuit

The driving factor of any Knudsen pump is the temperature difference across the nano porous membrane. Temperature profiles can be theoretically determined by creating a thermal circuit model [21]. In a thermal circuit Ohms law V=IR is re written as ΔT=QR (equation 2), where Q is the heat flow through the circuit, R is the thermal resistance, and ΔT is the temperature difference across the device. A cross section of the device is used to develop a thermal circuit for a device.

The thermal resistance R can be calculated by equation 3 and capacitance C by equation 4. The material properties and geometry of each device is used to calculate R and C. The thermal circuit is unique for each new design of the Knudsen pump and must therefore be analyzed individually utilizing these equations.

$$\Delta T = QR \tag{2}$$

$$R = \frac{Th}{A_C * \kappa} \tag{3}$$

$$C = m * c \tag{4}$$

Where Q is heat flow, R is thermal resistance, Th is thickness of material, A_C is the cross sectional area of the material the heat is flowing through and κ is the thermal conductivity of the material. C is the thermal capacitance, m is the mass of the material, and c is th specific heat capacity of the material.

Chapter 3: Device 1

The design of Device 1 included placing a Knudsen pump consisting of nanoporous membranes on top of a reservoir, creating an all in one device [22]. The whole device would be placed on the skin and the heat of the skin would travel through the device from the bottom plate to the fluid filled reservoir to the nanoporous material and power the Knudsen pump. Figure 3 shows the design of device 1. When the Knudsen pump is functioning, it pumps air into the reservoir and drives the pharmaceuticals out of the reservoir. Six devices were made this way to test different aspects that affect the function of the device. The thickness of the Knudsen pump affects the pressure that is generated; therefore placing a thicker Knudsen pump on the device should drive the water out at a lower temperature. The outlet pipe of the device represents a resistance to flow, so by using a larger diameter outlet pipe, less pressure would be needed for the
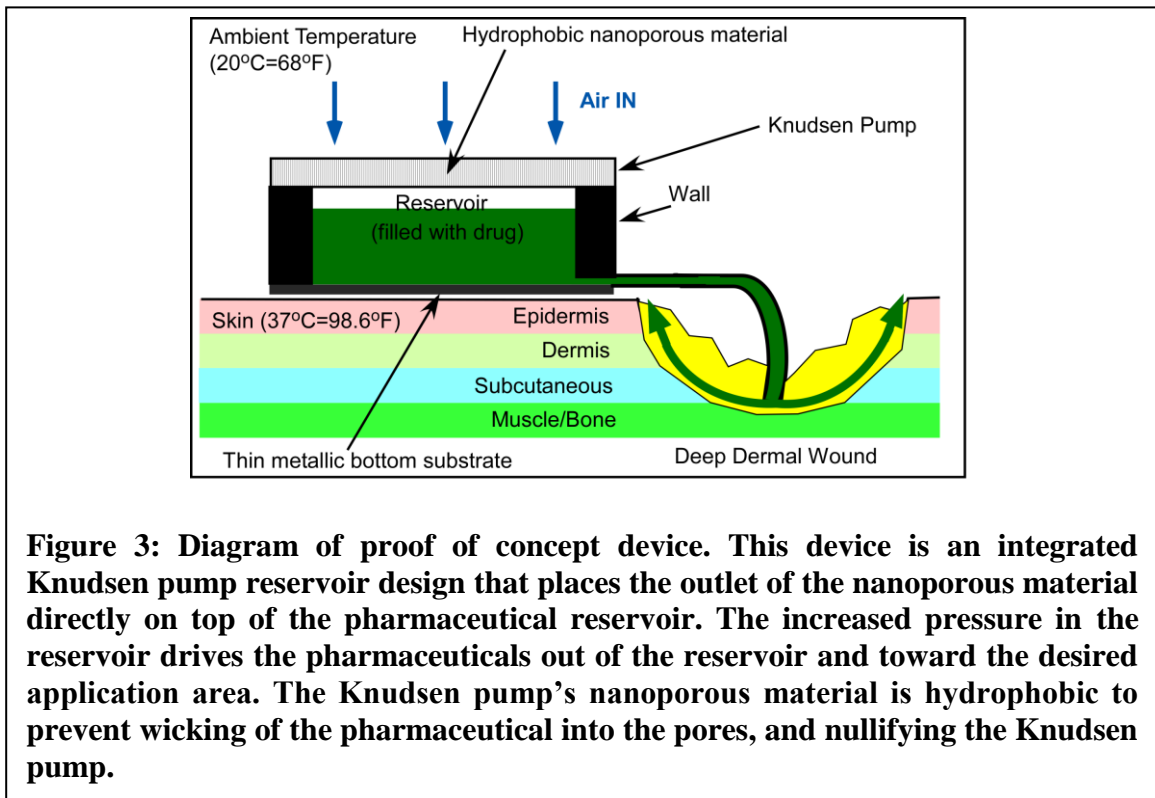
Figure 3: Diagram of proof of concept device. This device is an integrated Knudsen pump reservoir design that places the outlet of the nanoporous material directly on top of the pharmaceutical reservoir. The increased pressure in the reservoir drives the pharmaceuticals out of the reservoir and toward the desired application area. The Knudsen pump's nanoporous material is hydrophobic to prevent wicking of the pharmaceutical into the pores, and nullifying the Knudsen pump.

device to function. Four devices were made with two thicknesses of Knudsen pumps and two diameters of outlet pipes. The final two devices were controls in the experiment that varied the outlet pipe but the Knudsen pump was replaced with a mesh that is known to not work as a Knudsen pump. The purpose of the control devices was to show that there were no other phenomena causing the device to function.

Chapter 3.1: Thermal Circuit Analysis

The thermal circuit for this design is simple because the heat flows through the middle of the device. Figure 4 shows the thermal circuit used to analyze the device. Based on this thermal circuit the theoretical data from Figure 4, Figure 5 can be calculated and help determine the material properties that would work the best in the device. The problem with this thermal circuit is the dynamic nature of the reservoir. As time continues the amount of liquid in the reservoir changes and a new resistance is

Figure 4: Thermal Circuit for Device 1. The left figure represents the starting thermal circuit for the device, assuming a full reservoir. This is the circuit used to determine the best bottom substrate material. The right figure represents the thermal circuit after some fluid has left the reservoir. The air resistance increases and the water reservoir resistance decreases as fluid exits the reservoir.

Figure 5: Theoretical pressure generation of Knudsen pump of device 1 as a function of nanoporous material thickness. The material properties of the bottom substrate were varied to deteremine the best material to use for pressure generation. This figure shows that as the thickness of the nanoporous material increase so does the pressure, which is expected because the temperature difference will be greater. The figure also shows the relationship of thermal conductivity of bottom plate material to pressure generation. As the thermal conductivity of the bottom material increases so does the pressure generation. The thermal conductivity of copper is the greatest, followed by PTFE and last by PDMS which is the same relationship of which material lads to the greatest

introduced that increases as time goes on.

Chapter 3.2: Fabrication of Device 1

Device 1 was made to hold water until the Knudsen pump drives it out of the device. The Knudsen pump of the device was made from hydrophobic Sterlitech Polypropylene Membrane Filters to prevent the water wicking into the membrane. The walls of the device were made from a rubber gasket and the bottom of the device, which comes in contact with the heat source, is made from copper. Having a rubber gasket allowed for a syringe to be used to inject the water for testing. The copper bottom plate was selected to maximize the heat transfer to the Knudsen pump. Figure 5 shows the theoretical pressure that could be generated with varying the thickness of the nanoporous
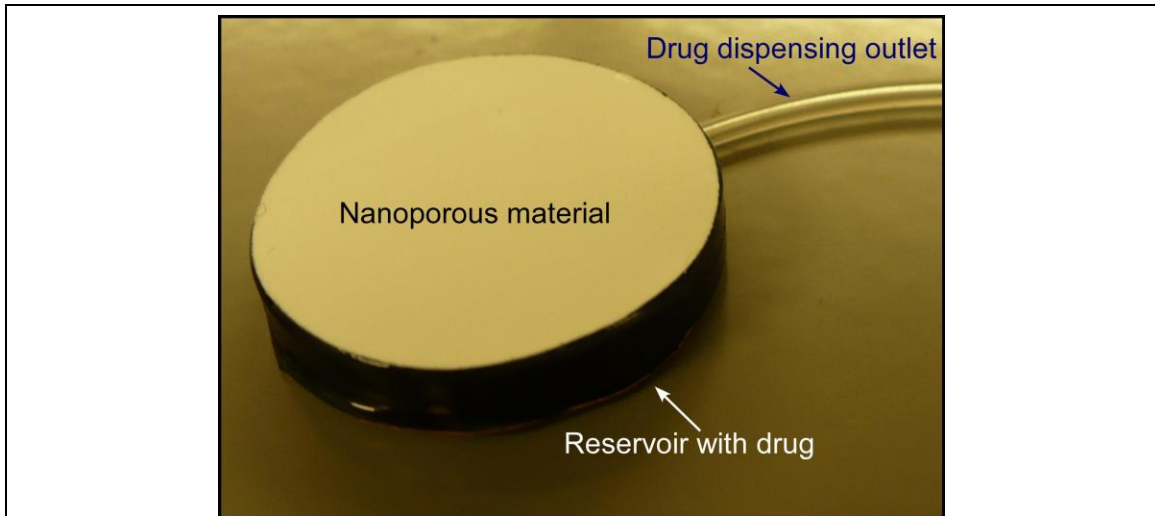
Figure 6: Picture of fabricated device 1. The white portion of the device is the nanoporous material that is the Knudsen pump of the device. The reservoir is created by placing the nanoporous material on a rubber gasket and closing the bottom with a copper sheet.

material and changing the material of the bottom plate. Figure 6 shows a picture of the fabricated device.

Chapter 3.3: Testing

The importance of the device 1 was proving that a Knudsen pump could be placed on the skin, and propels a fluid out of the reservoir. In order to determine if this was possible the device was placed on a resistive heater and the temperature was measured using a k type thermocouple; water was used as a replacement for pharmaceuticals during testing. The temperature was recorded at the time in which the water was released from the device. This temperature was deemed the threshold temperature and marked the minimum temperature needed for the device to operate. The flow rate from the device was also determined by measuring the time it took the water to move 1 cm and dividing that speed by the cross sectional area of the outlet tube.

Chapter 3.4: Results

As stated previously, six devices were created and tested to prove that a Knudsen pump could function as a pharmaceutical delivery device. Two of the devices were controls and instead of having a Knudsen pump on the top of the device, and polypropylene mesh was attached that will not work as a Knudsen pump. There were two variables in this testing, thickness of Knudsen pump and diameter of outlet pipe. As seen in Figure 7 the temperature was measured at the point in which the water was released from the reservoir. In the case of the two controls, the water began to boil before any evacuation occurred, which was expected. Device A was the thinner Knudsen pump with a smaller outlet pipe, it also began to boil during testing. The other three devices didn't reach a boiling point but a definite trend can be seen in the results. The device with the highest pressure generation and the largest outlet pipe (Device D), worked at the lowest

Figure 7: Bar graph representing Device 1 testing data. The x axis presents the six tested device and the y axis is temperature. The bar represents the threshold temperature for the devices. The two control devices and Device A boiled and therefore never truly functioned. A representative line for body temperature is superimposed on the graph to show that Devices C and D have a threshold temperature below that of human body temperature and therefore are successful.

heater temperature. Device B had the same thickness of Knudsen pump and therefore the same pressure generation, so the difference between the releasing temperatures can be explained by the difference in outlet pipe size. Therefore assuming that the correct outlet port size is used, and a thick enough Knudsen pump, the device will work if placed on the skin.

Table 1 illustrates the flow rate data for the proof of concept devices. Since the control devices did not function properly, the flow rate measured was zero. The same occurred for Device A. Device D had the highest flow rate with 2.6 ul/min followed by Device B with 1 ul/min. Device C had the lowest flow rate but still began to operate well before Device B.

Table I: Results from Device 1 testing. This table presents the flow rates for the six tested devices. The only devices that functioned were devices B, C, and D.

Device	Nanoporous Material Thickness	Tube Diameter	Measured Flow Rate
Control 1	N.A.	254 μm	0
A	105 μm	254 μm	0
B	525 μm	254 μm	1.0 μL/s
Control 2	N.A.	508 μm	0
C	105 μm	508 μm	0.23 μL/s
D	525 μm	508 μm	2.6 μL/s

Chapter 3.5: Conclusions and Discussion

There were a few problems with the Device 1. The first major problem is the inconsistency of pressure generation. As the pharmaceuticals are driven out of the reservoir, the heat flow through the device changes, less heat gets to the Knudsen pump because of an increasing resistance due to air. Assuming a simple thermal circuit with three thermal resistances for Device 1, as soon as air enters the reservoir a fourth resistor is created that accounts for the air. As the quantity of the air gets larger the resistance increases and as the fluid of the reservoir leaves that resistance decreases. For the device to work properly the resistance of the bottom plate and the Knudsen pump needs to be as small as possible so the heat gets to the nanoporous material. The resistance of air is far greater than the resistance of water so as the reservoir is depleted the resistance that needs to be small actually increases.

Another potential problem is the small size of the reservoir. The reservoir should be around 25 mL to sustain potential therapies, and this design has a much smaller reservoir capacity. The final problem is the inability to compound pressure. If larger pressures are needed to drive the pharmaceuticals, for instance with a larger reservoir, this design does not allow for multiple pumps to be put in series, which would increase the pressure. All of these concerns are addressed in the second iteration of the device.

Chapter 4: Device 2

In order to address concerns with the Device 1 design, it was redesigned [23]. Design 2 separated the Knudsen pump from the reservoir and places it directly on the skin, as seen in Figure 8. Air then flows from the Knudsen pump to the reservoir and drives the pharmaceuticals from the reservoir to the patient. This design allows for greater pressure generation from the Knudsen pump, as well as a more consistent

Figure 8: Diagram of redesign device presuming application of dermal wound drug delivery. This design cascades the Knudsen pump to the reservoir and allows for direct contact of the Knudsen pump to the skin. The closer proximity to the heat source provides a greater temperature difference for the Knudsen pump and therefore a better pressure difference. The freedom of the Knudsen pump from the reservoir also allows for the Knudsen pump to be placed in series with more Knudsen pump to create more pressure if needed.

pressure generation. Figure 9 shows how the air travels through the new Knudsen pump design. Since the Knudsen pump is no longer dependent on the heat flow through the reservoir it is substantially more consistent, because the thermal circuit does not change. Also, the Knudsen pump is separated from the reservoir, allowing for the device pressure generation to be compounded before being sent to the reservoir.

Figure 9: Diagram depicting the glue layout of the Knudsen pump portion of the redesign device. This view of the device shows how the air travels through the device. The glue on the top and bottom of the nanoporous material is only applied to three sides, leaving a side open for air to travel. These sides are opposite to one another to allow for the air to enter the bottom left of the nanoporous material and leave from the top right. This manipulation of air travel is essential to creating a working Knudsen pump.

Chapter 4.1: Thermal Circuit Analysis

To estimate the temperature difference and therefore pressure difference across only the Knudsen pump of the thermal circuit, we determine the thermal resistance, thermal capacitance, and heat flow through the whole device. The thermal resistance and capacitance of the Knudsen pump is a material property and independent of the conformation of the device. The heat flow (Q) through the Knudsen pump is dependent of the geometry of the device and therefore the thermal resistance and capacitance of every other piece of the device must be determined, and the whole thermal circuit must be analyzed to determine the heat flow. In order to fully analyze the circuit the circuit analyzing program Multisim is used. Figure 10 shows the circuit that was used in the program. A DC power source was connected to the heat sink and the stainless steel
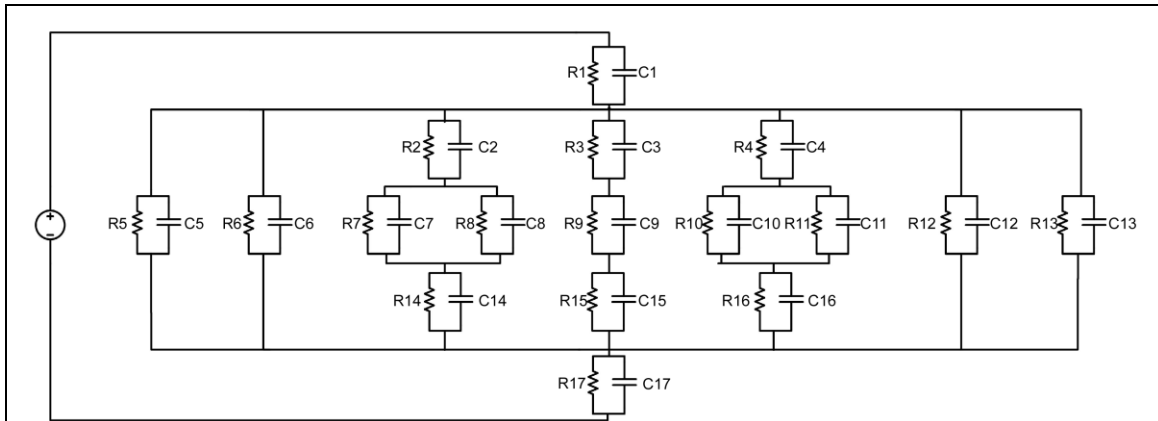
Figure 10: Thermal circuit used in Labview Multisim. There are 17 resistors and 17 capacitors within the circuit. The DC power source provides the temperature difference across the whole device and is assumed to be 8 V. R8 and C8 are the resistor and capacitor elements that represent the nanoporous material of the Knudsen pump and voltage difference (temperature difference) across these elements are what is analyzed in this simulation.

portions of the model. The circuit was analyzed by measuring the voltage over time, across the nanoporous material of the Knudsen pump. Figure 12 gives the results of the transient analysis of the thermal circuit. This data is superimposed over actual pressure data discussed in chapter 4 and Figure 18. The simulation results are not on the same scale as the pressure data, but qualitatively the simulation is a good representation of what is to be expected from the Knudsen pumps. It is to be expected that there will be an overshoot of temperature difference before the temperature difference comes to an equilibrium. As you can see in Figure 11 this is exactly what happens in the experimental data.
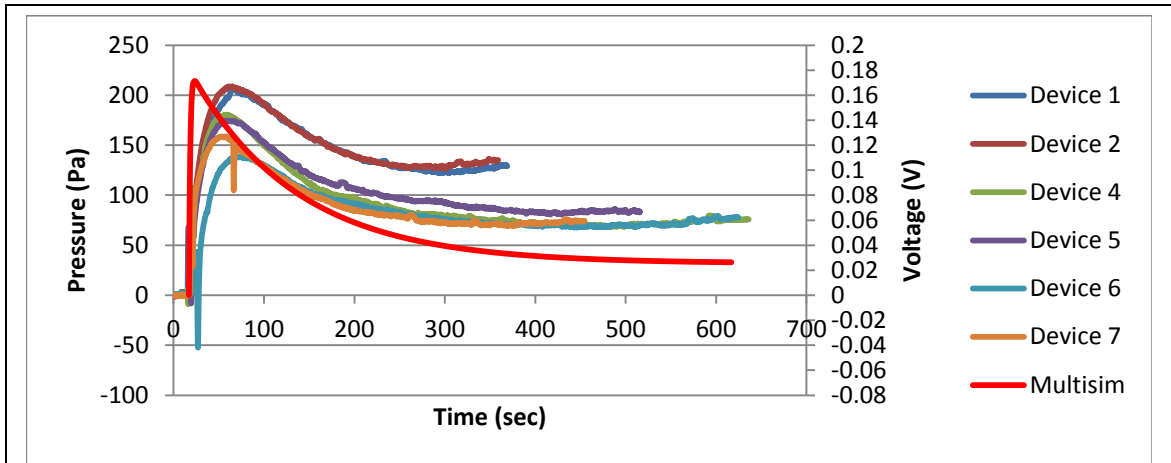
Figure 11: Experimental pressure data with Multisim simulation data overlay. The Solid red line represents the Multisim simulation data. This data shows the relative temperature response of the device when placed on the skin. This qualitative data shows that the temperature will increase across the nanoporous material sharply and then settle overtime to a steady state, which based on equation 1 we know directly correlates to a steady state pressure. This graph also presents data from experimental measurements of Knudsen pumps and shows that the simulation is correct and that there is a peak that occurs before the device comes to a steady state temperature and pressure.

Chapter 4.2: Fabrication

Device 2 moved the Knudsen pump from atop the reservoir to directly on the skin. The second iteration of the device focuses on biocompatibility by replacing the copper of the proof of concept device with a more compatible type 304 stainless steel. Since the Knudsen pump does not come in contact with a liquid, the membranes used in the pump do not have to be hydrophobic. Removing the limitation of hydrophobicity allowed for a decrease in pore size and as we know from Knudsen pump theory this leads to an increase in pressure. A common heat sink is added to the top of the device to allow for a more efficient cooling on the cold side of the device. Figure 12 shows a picture of the fabricated device.
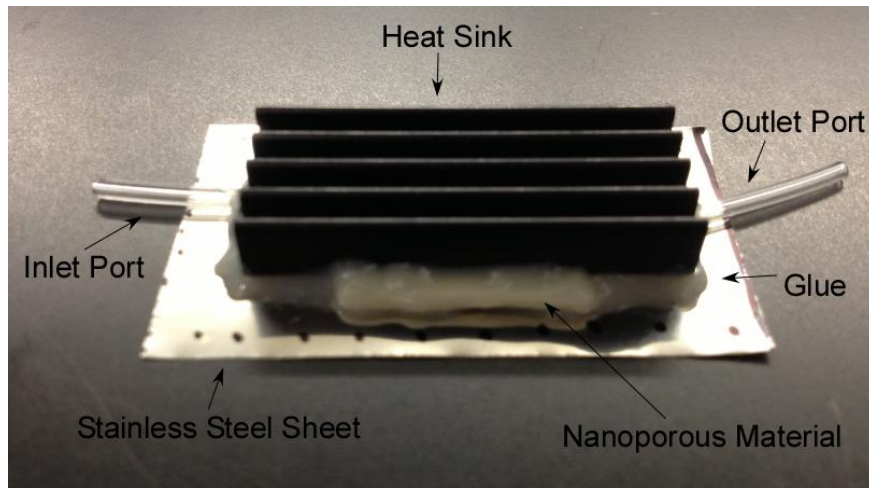
Figure 12: Photograph of fabricated device 2. This photograph shows the location of the inlet and outlet ports in relation to the nanoporous material. It also gives a representation of the glue that is used to create the pump and how much used. The stainless steel used to create the device is type 304 stainless steel.

Chapter 4.3: Testing

Two measurements are needed to analyze the new design of the pump, max pressure and flow rate. The pressure was measured by connecting the Knudsen pump to a pressure sensor and powering the device. The pressure was then subtracted from the ambient pressure to determine the pressure difference. The device was powered two ways; first by placing it on a forearm to prove that the device can be human powered. The second way was using a resistive heater to simulate the human arm pictured in Figure 16.

The flow rate was measured by applying a separate flow rate via a syringe pump, and measuring the corresponding pressure as illustrated in Figure 13. Figure 14 is a representative graph to show how the flow rate is calculated via pressure versus flow rate curve. The maximum flow rate is when there is no pressure in the system. The pressure is measured with at least two set flow rates, plotted, and a line is graphed. The Y-intercept of this line is the max flow rate of the device.

Figure 13: Schematic of flow rate measurement system. Air input comes from the syringe pump and is pumped out of the system by the Knudsen pump. When the flow rate of the syringe pump is equal to the flow rate of the Knudsen pump the pressure difference between the pressure sensor and the ambient pressure will be zero.
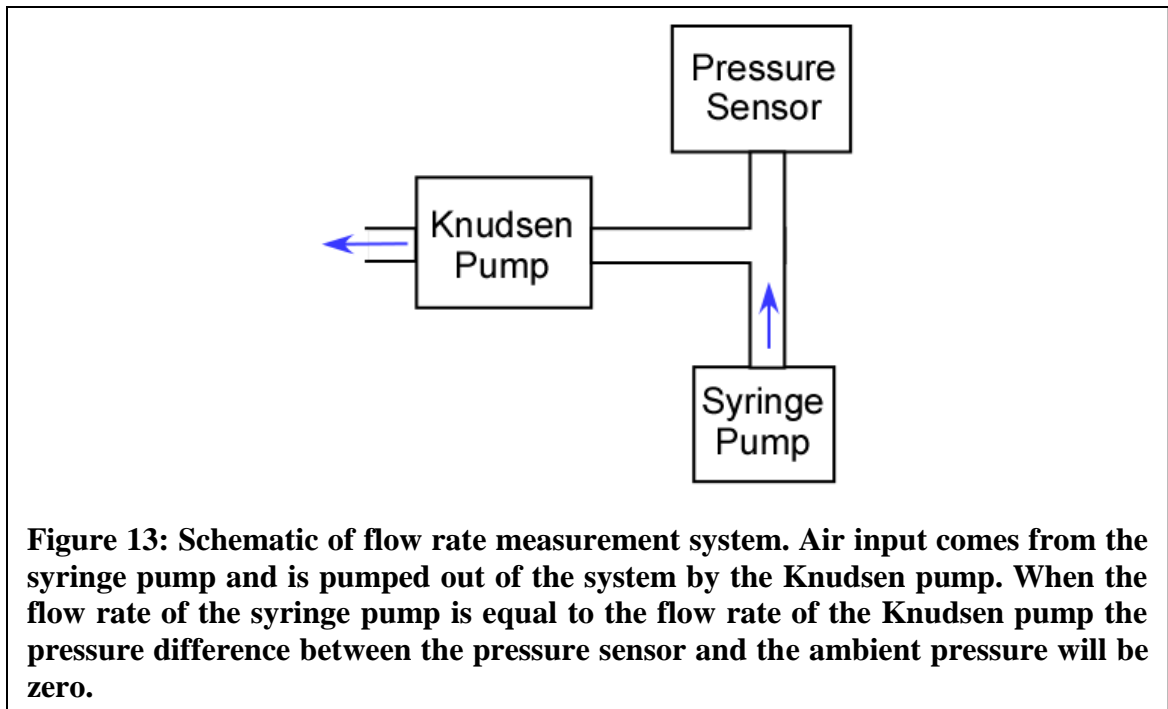
The final testing of Device 2 was to quantify the effect of attaching individual Knudsen pumps in series has on pressure generation, and placing the devices in parallel on the flow rate. The devices are placed in series by attaching the output on the first pump to the inlet of the second and so on. This effectively compounds the pressure generated. The same can be said for the flow rate with devices in parallel. By connecting all of the outlets of the devices together the cross sectional area of the Knudsen pump is increased which increases the amount of pores that the air can go through, and increase the flow rate.
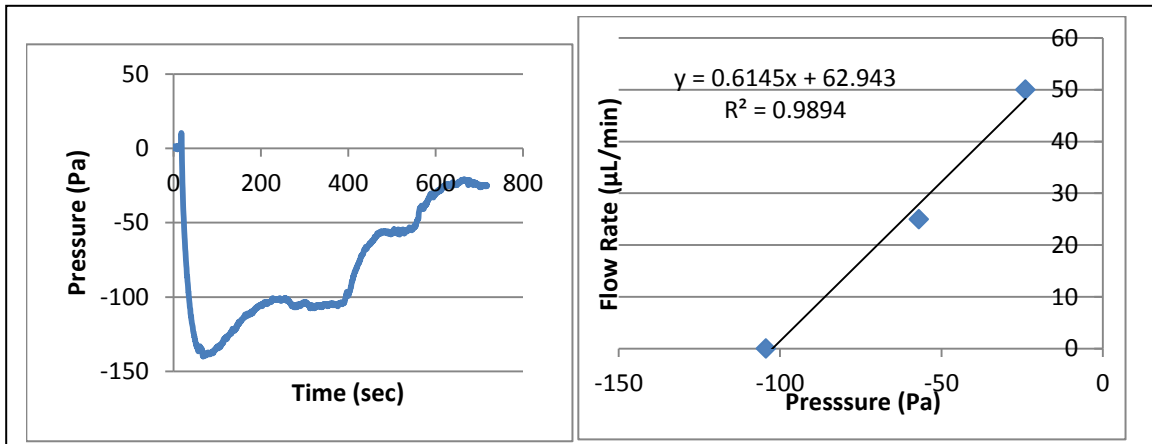
Figure 14: Representative flow rate calculation example. The left graph shows the pressure generation from the device being tested. The pressure is allowed to come to rest at 104 Pa. This pressure becomes the starting point for the flow rate calculation. A maximum pressure occurs at a flow rate of 0 and as seen on the right graph a point is placed at the location (-104,0). The second point on the right graph is obtained by applying a flow rate of 25 µL/min to the device and measuring the pressure, creating the point (-57,25). The third point is created the same way with a flow rate of 50 µl/min (-24, 50). Linear regression gives the final equation of flow rate given pressure. Just as the maximum pressure occurs at a flow rate of 0, so does a maximum flow rate occur at a pressure of 0. This equation is derived for every tested device and is used to determine the maximum flow rate of the device.

Figure 15 shows the testing setup for the series and parallel testing. All of the devices were placed on a resistive heater strip to simulate the human arm. Figure 16 shows the temperature profile of the heater strip and a human arm to illustrate that the temperature variation within the strip is similar to the arm and therefore it is an adequate human model to use for testing. This testing setup allows for consistent testing of the devices.

Chapter 4.4: Results

Since the Knudsen pump is placed directly on the skin in Device 2 there is a larger amount of heat reaching the nano porous material and therefore a greater pressure is generated by the Knudsen pump. This new design also makes the device easier to harness the pressure, allowing for multiple devices to be placed in series and parallel
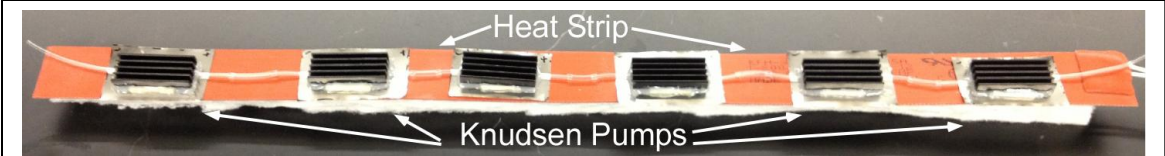
Figure 15: Photograph of series and parallel testing set up. The heat strip is a resistive heater powered by a DC power supply. Its length allows for up to six Knudsen pumps to be tested at once.

easier. Figure 17 shows the pressure generation of two devices, one with a heat sink and one without, to determine the effectiveness of adding a heat sink to the top of the device. Adding the heat sink to the device not only increased the pressure generation but also lengthened the settling time of the device. Therefore the most efficient design of the device includes a heat sink to dissipate the accumulating heat.
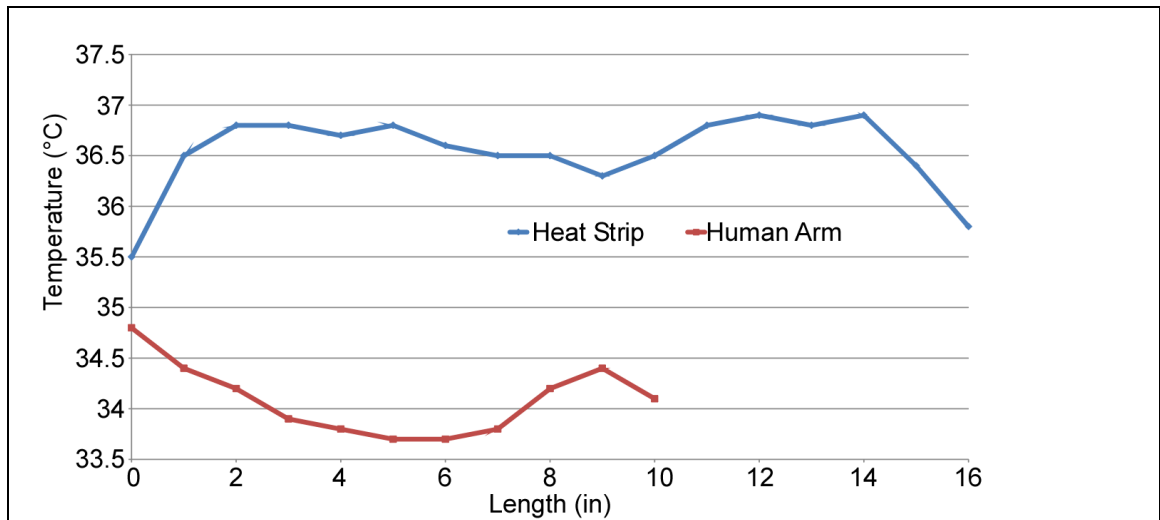
Figure 16: Temperature profile comparing the heat strip for testing and the human arm. This profile is used to determine that the heat strip is an adequate human model for testing.
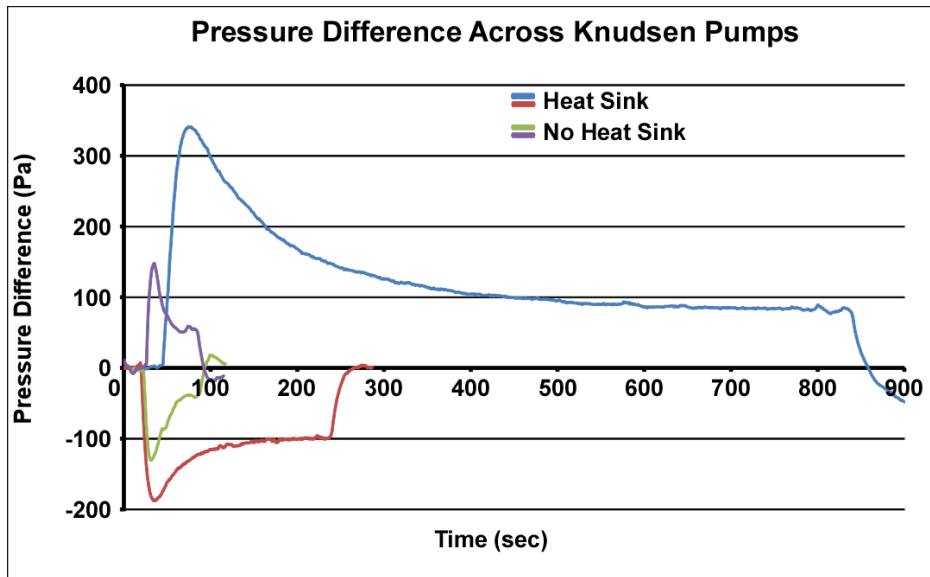
Figure 17: Comparison between pressure generation of device with and without a heat sink. The pressure lines for the device without a heat sink are substantially smaller for duration and max pressure. This is due to limited heat dissipation. Since heat sinks are made to dissipate heat efficiently, using them to create the Knudsen pump increases the max pressure and time response of the device.

Next, several devices were created to test how the device works when placed in
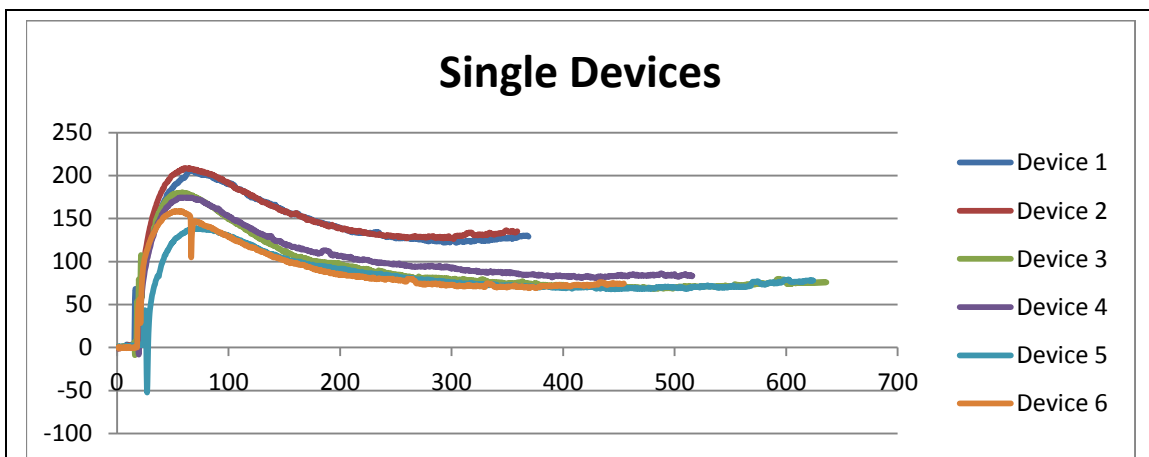
Figure 18: Pressure generation by single devices. Six devices were made and tested. Due to slight differences in fabrication Devices 1 and 2 outperformed the other four devices.

series and in parallel. Figure 18 shows the pressure difference measured for the six individual pumps. The variations in the pressure differences are due to small variations in the dimensions of each device. Figure 20 shows the pressure difference data for multiple devices connected in series. The devices were named in such a way that represents which devices were connected. For instance Device 1.2 means Device 1 is connected to Device 2. Based on equation 1 it is known that by having two stages in series the total pressure created by the devices is greater [24]. Figure 19 shows that this is the case and the increase in pressure is nearly double.

The devices were also tested in series with up to six devices. Figure 20 shows the pressure data for all of the series devices from two to six, and includes the single devices for comparison. As expected the pressure generated by the devices increases as the number of devices in series increases. Figure 18 shows the max pressure generated by
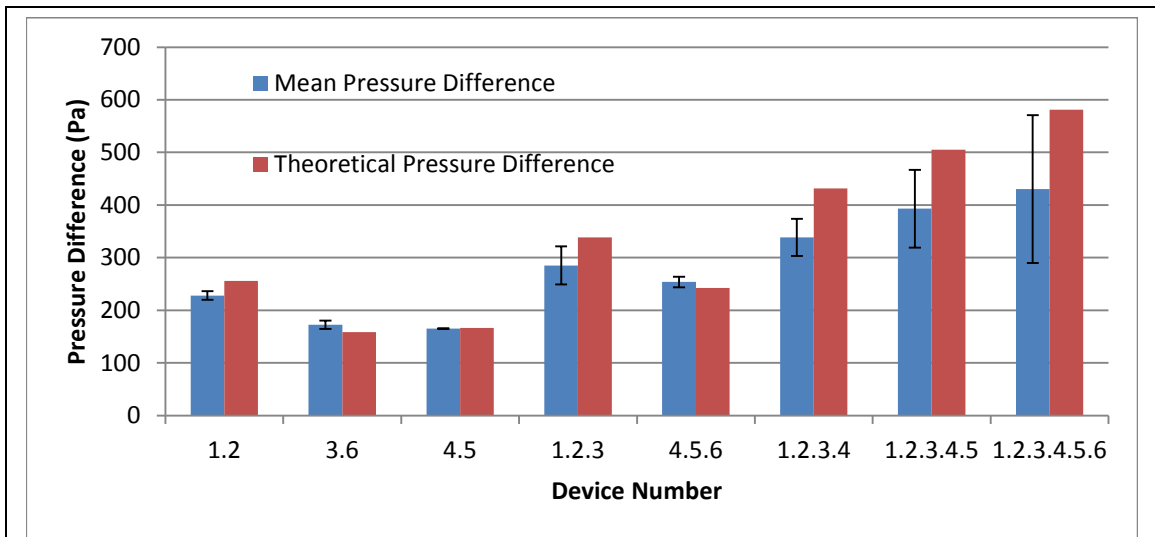
Figure 19: Bar graph of pressure generation of tested device compared to theoretical pressure. To determine the theoretical pressure that the series devices should achieve the single device pressures were summed in accordance to their series requirements. For instance the theoretical pressure for device 1.2 is the sum of the pressure generated by devices 1 and 2. The measure pressures were off by a maximum of 10%.

each device, and here you can see the upward trend better. A few anomalies are the devices 1 and 2. Individually the devices produced a larger pressure than the other single devices likely due to variations in construction, and when placed in series these devices outperform the other devices. For instance, Device 1.2 produces much larger pressure than Devices 3.6 or 4.5 even though they have the same number of devices in series. The flow rates were also measured for the series devices and provided an interesting discovery. It was believed that an increase in the number of devices in series would decrease the flow rate, due to an increased resistance to flow. As seen in Figure 19 this is not the case. The flow rate stays consistent with the more devices that are added on with a mean of 73.5 µL/min. This is a promising aspect of the devices assuming that a particular flow rate and pressure is needed to operate the reservoir there is not a negative effect on
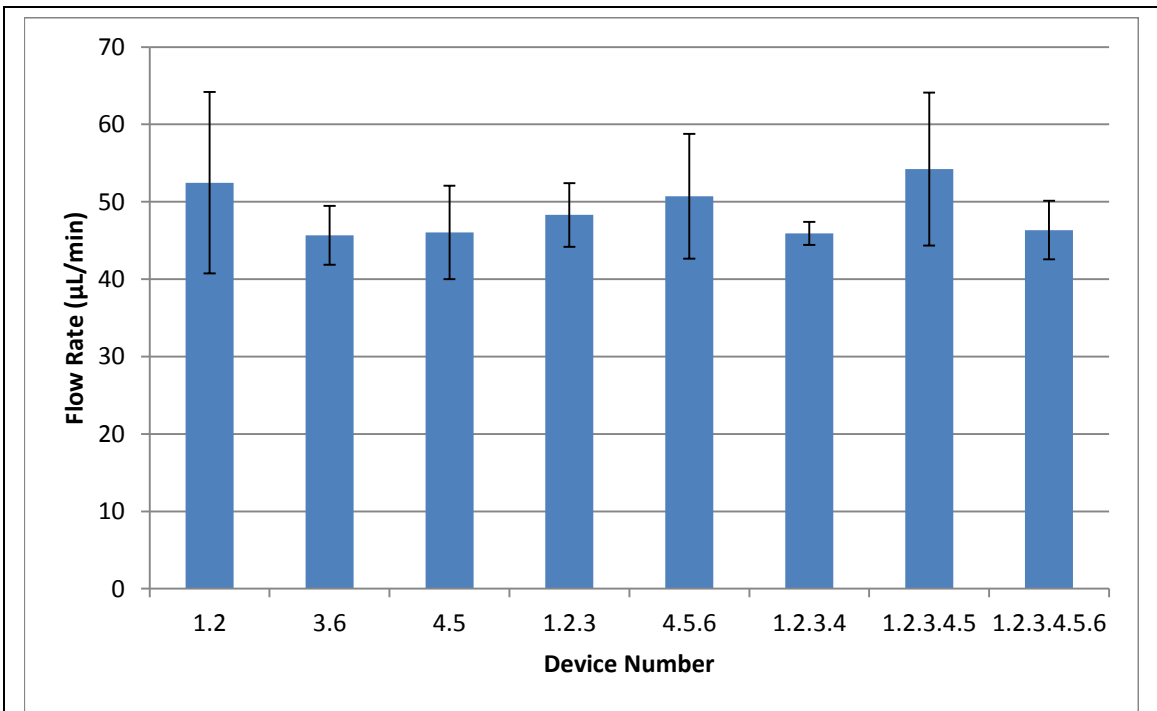
Figure 20: Bar graph of flow rate measurements for the series devices. The flow rate for series device is expected to reduce as the number of devices in series increases. As we can see by the bar graph, the flow rates remain relatively the same.

flow rate in relation to pressure generation.

The final stage of testing of Device 2 was to measure the effect of adding pumps in parallel on flow rate and secondarily on pressure generation. In the testing section it is discussed how the flow rate was measured and Figure 21 displays the flow rates for all of the devices. The flow rate for individual pumps averages 71 µL/min more than doubles when two devices are placed in parallel. After that the flow rate stabilizes at 190 µL/min for 2, 3, and 4 devices in parallel. When 5 devices are measured the flow rate jumps to 350 µL/min and then stabilizes again.

Chapter 4.5: Conclusions and Discussion

Device 2 was a successful design of the Knudsen pump. It solves the problem of
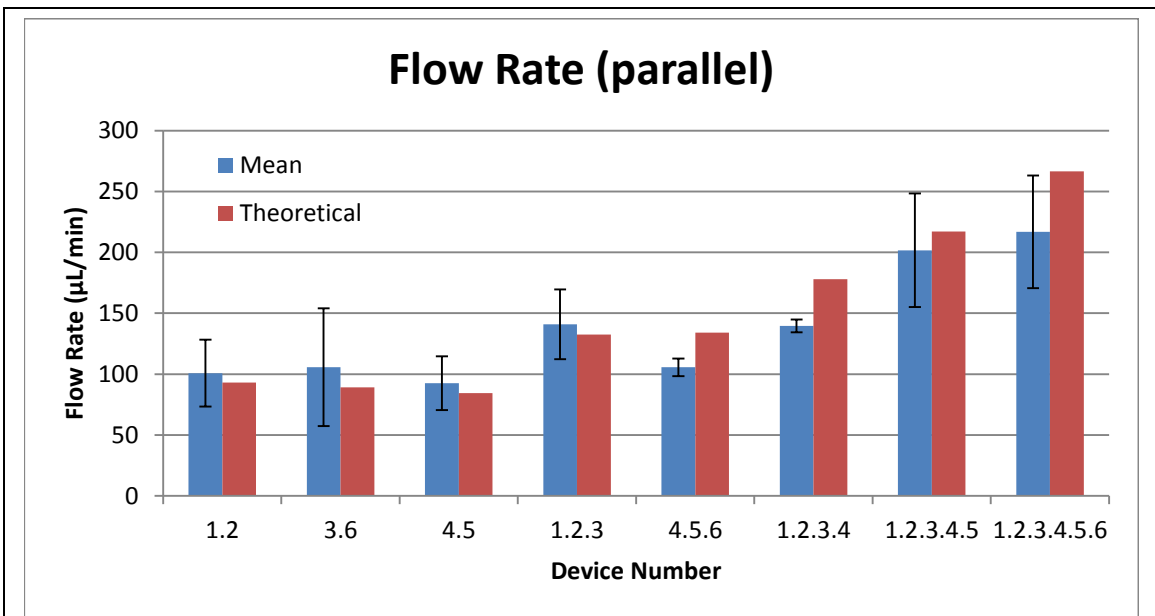
Figure 21: Experimental flow rate data from parallel device testing. The theoretical flow rates are estimated much like the theoretical pressures of Figure 19. For Device 1.2 the flow rate of device 1 was added to the flow rate of device 2 to determine the theoretical flow rate. The experimental was off by at most 51% but the general upward trend can be seen which is expected.
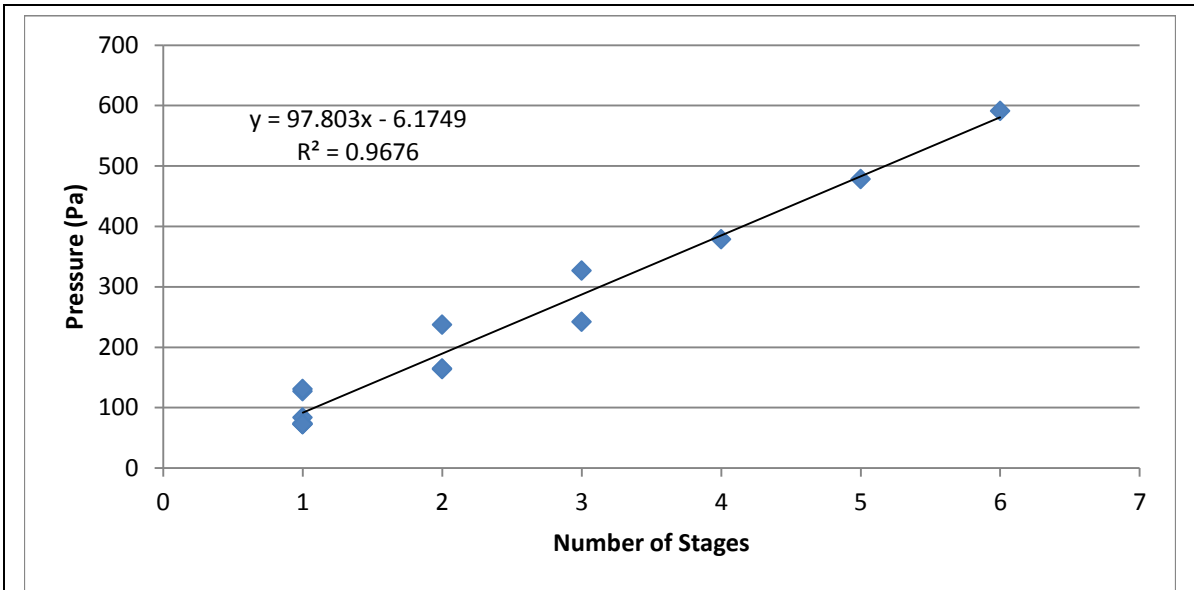
Figure 22: Pressure vs number of stages graph. This graph and resulting linear regression equation can be used to determine the number of stages needed to generate a particular pressure. This information is used after the reservoir testing to design the final device.

not being able to be cascaded that Device1 had, and being placed directly on the skin allows for greater pressure generation. The results of series pressure testing can be analyzed to determine a relationship between number of stages and pressure generation. This is done by plotting the pressure generation of each device as a function of stages. The results are graphed in Figure 22.
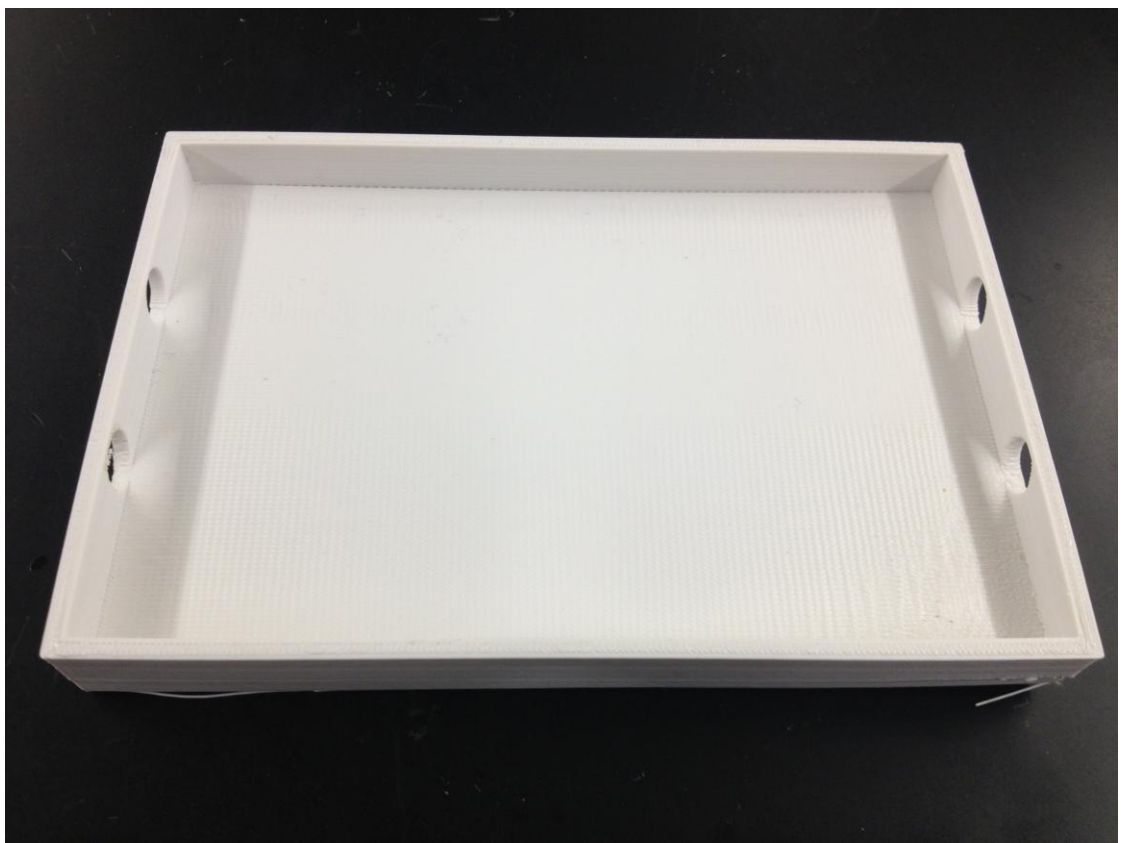
Figure 23: Photograph of printed reservoir box. The box was printed using a Replicator 3D printer in ABS plastic. The holes on the left are outlet holes for the IV bags connectors to fit through and the holes on the right are the inlet holes for the second IV bag. The box was closed off by clamping a plastic sheet over the open area

Chapter 5: Reservoir

Based on Device 2 the Knudsen pump is used to supply air to a pharmaceutical reservoir. This reservoir facilitates the buildup of pneumatic pressure from the Knudsen pump and allows the pressure to be transferred to the pharmaceuticals.

Chapter 5.1: Fabrication

The reservoir consists of a box, pictured in Figure 23, with two plastic IV bags inside. One bag holds the pharmaceuticals intended for the patient, and the second bag is empty. The second bag is connected to the Knudsen pump, and fills with air. As the

second bag fills with air it applies pressure to the first bag, driving the pharmaceuticals out. The box is made from ABS plastic, intended to be strong enough to withstand the building pressure from the Knudsen pump. The rigidity of the box also protects the pharmaceutical bag from being pressed accidentally and releasing the medicine too soon. The reservoir box is intended to be worn, making the infusion pump a very portable device.

Chapter 5.2: Testing

The reservoir requires a certain pressure to operate, which needed to be determined. In order to do this, the pharmaceutical bag was filled with water and a tube

Figure 24: Block diagram of reservoir testing setup. The reservoir is oriented so the water is exiting the box downward and the traveling up the tube and coming to a hydrostatic starting point. The testing starts from this point and measures for far the water move up from the starting point.
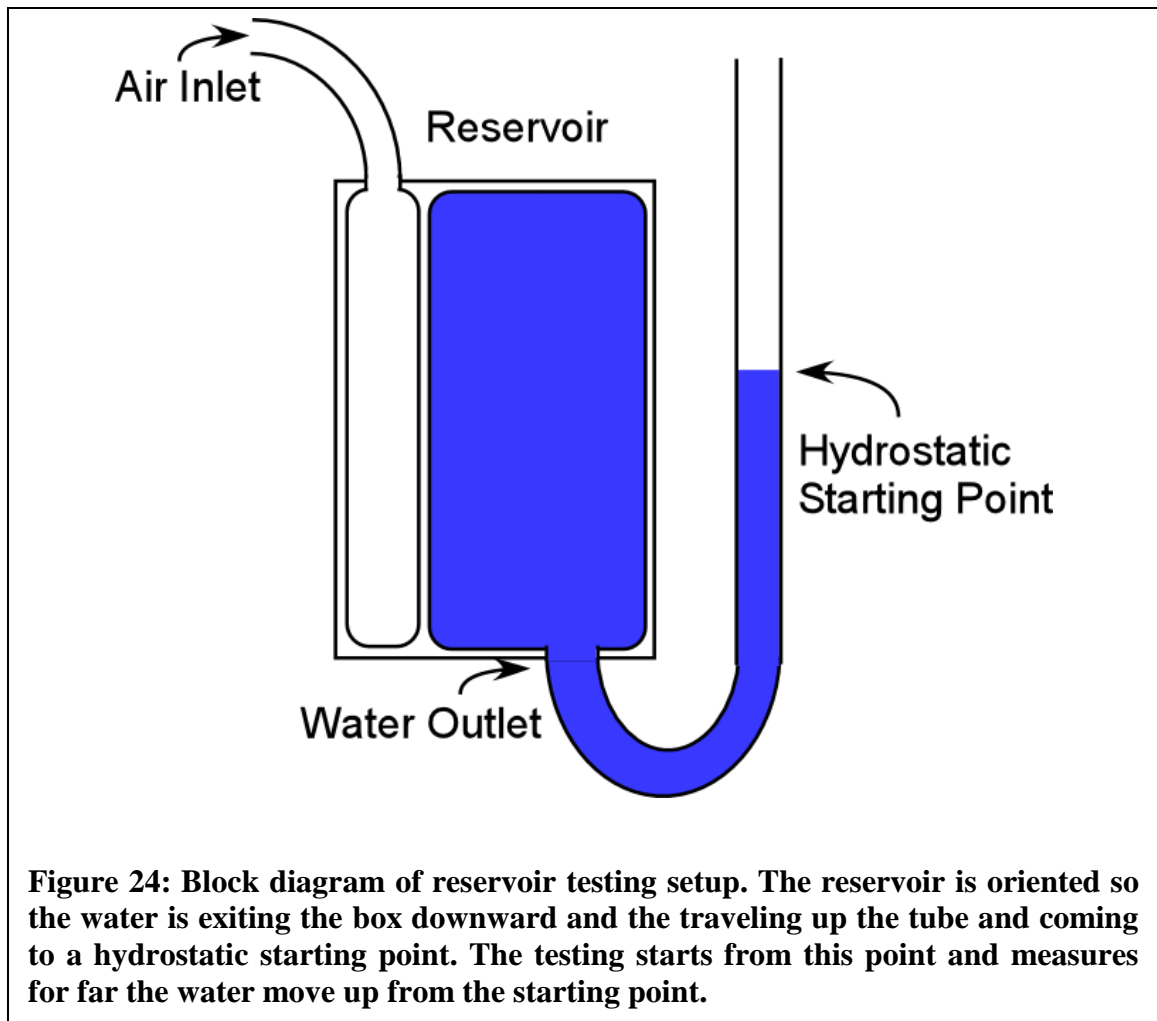
was attached to the air bag. As seen in Figure 24 the reservoir was oriented so the water was flowing downward with gravity, and then the outlet tube was directed upward. The water came to a hydrostatic level with the reservoir and this marked the starting point of the testing. Pressure was applied to the air bag by blowing into the inlet tube. The air was blown into the bag until the water from the pharmaceutical bag began to rise in the outlet tube. The pressure required to move the water was measured as well as the pressure required to maintain a specific water level. The reason the testing was oriented upward is to account for a worst case scenario.

Chapter 5.3: Results

The pressure required to move propel the fluid from the reservoir is shown in Figure 22. There is a positive correlation between the distance the water traveled and the pressure required to move the water. This is to be expected because of the greater height results in a greater potential energy that needs to be overcome. The resulting linear equation of the data can help determine how much pressure is needed to move a certain distance.

Chapter 5.4: Conclusions and Discussion

Based on the equation in Figure 25, and the equation in Figure 22 a new equation can be created to determine the number of stages needed to move the fluid from the reservoir a certain distance. These equations are re written below.

$$Pressure\ (Pa) = 97.803\ (\#\ of\ Stages) - 6.1749 \qquad (5)$$

$$Pressure\ (Pa) = 80.508\ (Distance\ cm) + 1002.3 \qquad (6)$$

$$\#\ of\ Stages = 0.8232\ (Distance\ cm) + 10.3113 \qquad (7)$$
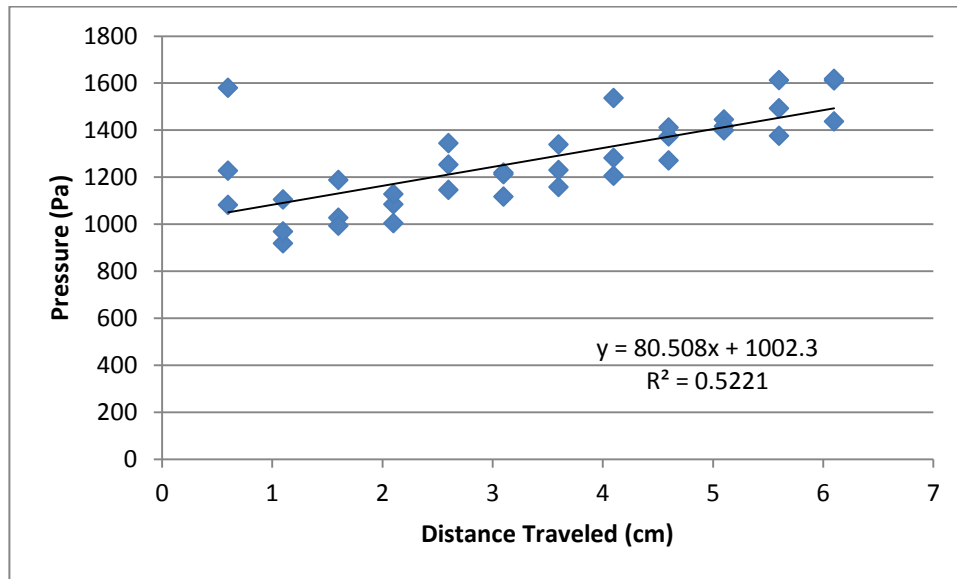
Figure 25: Reservoir testing data. The x axis represents the distance the water traveled and the y axis represents the pressure required for the water to travel that distance. The experiment was performed three times to determine the relationship between distance traveled and pressure.

Chapter 6: Device 3

The final device has the same design as Device 2 but with the exact number of stages of the Knudsen pump needed to operate the reservoir to a certain distance. Equation 8 expresses the number of stages needed in terms of distance to move the fluid. The distance of 10 cm is used to determine the number of stages needed for the final device. Using a 10 cm distance 18.5433 stages are needed which is rounded to 19 stages.

Chapter 6.1: Fabrication

The final Knudsen pump was made with the same materials as the second design Knudsen pump, because that has been proven to be the most efficient thus far. 19 stages were created with the same method as Device 2.

Chapter 6.2: Testing

The last stage of testing determined if the final Knudsen pump works with the reservoir. The final test consisted of placing the 19 stage Knudsen pump on a resistive heater and attached to the reservoir. The final design will be considered a success if the Knudsen pump operates the reservoir. A total of 24 devices were created, of the 24 created only 14 functioned properly in series. Based on equation 7, this should yield a distance of 4.48 mm.

Chapter 6.3: Results
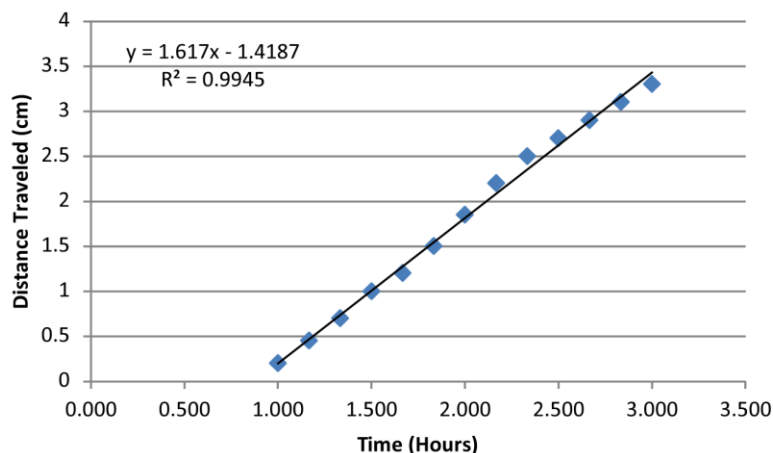
Figure 26: Graph of experimental results from device 3 testing. The graph displays the distance the fluid travels from the reservoir over time. The slope of the trend line represents the velocity of the fluid leaving the reservoir.

The 14 stage device was connected to the reservoir and pressure sensor. The level of the fluid from the reservoir, and the pressure were noted every ten minutes for 3 hours. Figure 27 displays the distance the fluid traveled from the reservoir over time. The linear trend line from the graph displays the velocity of the fluid from the reservoir, and by multiplying by the cross sectional area of the tube the volumetric flow rate can be calculated. The velocity from the graph is 1.617 cm/hour, and the cross sectional area of the tube is 0.00456 cm^2, the flow rate is then 7.37 µL/hour.

Since the distance the fluid traveled in experimentation is much different from the theoretical estimation, Figure 28 displays the pressure versus distance from the experiment. This data can be used as a better estimate for how much pressure is needed to move the fluid. The y intercept of the linear trend from Figure 28 is the minimum pressure necessary to propel a fluid from the reservoir.

32
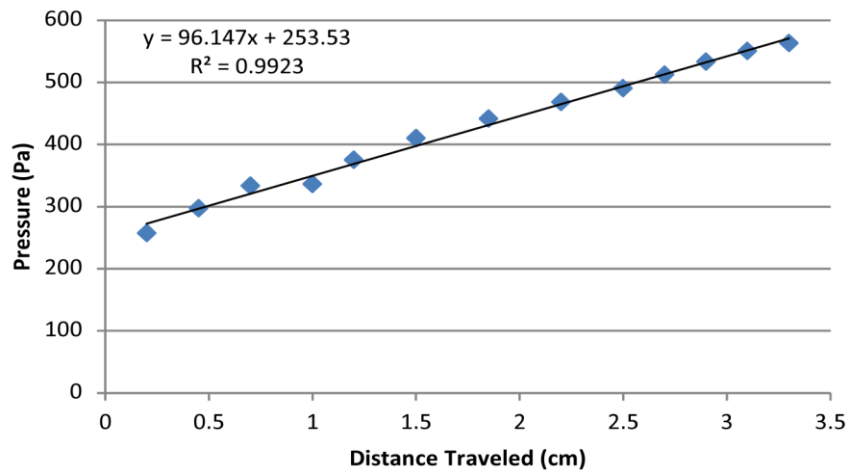
Figure 27: Pressure versus distance traveled data from device 3 testing. This data can be used to further develop the human powered Knudsen pump for the infusion pump.

Chapter 6.4: Conclusions and Discussion

Even though the 14 stage did not drive the fluid a full 10 cm, the device did propel the fluid over 3 cm. The device successfully moved a fluid from the reservoir, and with the new knowledge of the pressure required to move the fluid a certain distance, a human powered Knudsen pump can be custom made to deliver a fluid any specified distance.

Chapter 7: Discussion and Conclusions

Two infusion pumps, each utilizing human powered Knudsen pumps, were created and tested in this study. The first device integrated a human powered Knudsen pump with a pharmaceutical reservoir and the second device cascaded a human powered Knudsen pump with a pharmaceutical reservoir. The first device was tested by measuring at what temperature the device began to function. Two devices were created with this design that functioned below body temperature. The second device was able to be manipulated by placing devices in series and parallel to increase the pressure and flow rate, respectively. This was proven in testing and a final device was created integrating the second Knudsen pump design with a pharmaceutical reservoir. The final device operated at a flow rate of approximately 7 microliters per hour.

In this study, the task of creating a human powered Knudsen pump based infusion pump was achieved. This was completed using the first device design and later improved upon with the second device design. The characterization of the second device design was accomplished, allowing the creation of a Knudsen pump with a specified pressure and flow rate dependent upon the needs of the pharmaceutical reservoir.

Chapter 7.1: Limitations

There are several limitations to both the device design and testing scenarios described in this work. The design of Device 2 improves upon Device 1, but is not as efficient as it could be. The Knudsen pump portion of the device could be smaller, therefore allowing for more devices to be placed in series and subsequently lead to an increase in the pressure generation. The fabrication of the device can lead to variations in the geometries of the different devices, which is why the single stage data is different for

each fabricated device. With improvements to the design, it is possible to limit these differentiations. Other limitations occur with the testing of the devices as the testing did not occur directly on human skin, but on a resistive heater. The heater is set up to provide a similar temperature as that found on human skin, however there remains a slight temperature difference.

Chapter 7.2: Future Work

The future work of this project would be directed at addressing the limitations of this research. A new design would be necessary to limit the variations between different fabricated devices and improve the pressure generation. Also, this future device would need to be tested fully on human skin to prove that the device is human powered throughout the testing process. More work should also be done to determine what the working conditions of the final product would be, such as flow rate. Overall, the future work would be aimed towards finalizing a device for use in the administration of pharmaceuticals to dermal wounds. Lastly, the device needs to be characterized based upon the output flow rate from the reservoir. For instance, is there a correlation between Knudsen pump pressure and reservoir flow rate or Knudsen pump flow rate and reservoir flow rate? With all of these future tests, a novel approach to pharmaceutical delivery can be successfully achieved.

References

1.	Tallon RW. Infusion pumps. Nursing management. 1996;27(12):44-6. English.
2.	FDA U. White Paper: Infusion Pump Improvement Initiative. In: Health CfDaR, editor.
http://www.fda.gov/medicaldevices/productsandmedicalprocedures/GeneralHospitalDevicesandSupplies/InfusionPumps/ucm205424.htm2012.
3.	Baumann D. Effect of flow on human endothelial cell and dermal cell growth rates supplemented with drug infused media 2012. Available from: http://digital.library.louisville.edu/cdm/ref/collection/etd/id/2380.
4.	Madden JW, Peacock EE, Jr. Studies on the biology of collagen during wound healing. 3. Dynamic metabolism of scar collagen and remodeling of dermal wounds. Annals of surgery. 1971 Sep;174(3):511-20. PubMed PMID: 5111290. Pubmed Central PMCID: PMC1397578. Epub 1971/09/01. eng.
5.	Staas Jr. WE, Cioschi HM. Pressure sores - a multifaceted approach to prevention and treatment. Western Journal of Medicine. 1991;154(5):539-44.
6.	Boateng JS, Matthews KH, Stevens HNE, Eccleston GM. Wound healing dressings and drug delivery systems: A review. Journal of Pharmaceutical Sciences. 2008;97(8):2892-923.
7.	Rizzi SC, Upton Z, Bott K, Dargaville TR. Recent advances in dermal wound healing: biomedical device approaches. Expert review of medical devices. 2010 Jan;7(1):143-54. PubMed PMID: 20021245. Epub 2009/12/22. eng.
8.	Chiang B, Essick E, Ehringer W, Murphree S, Hauck MA, Li M, et al. Enhancing skin wound healing by direct delivery of intracellular adenosine triphosphate. The American Journal of Surgery. 2007 2//;193(2):213-8.
9.	Hobson JP, Salzman DB. Review of pumping by thermal molecular pressure. Journal of Vacuum Science & Technology A: Vacuum, Surfaces, and Films. 2000;18(4):1758-65.
10.	Muntz EP, Sone Y, Aoki K, Vargo S, Young M. Performance analysis and optimization considerations for a Knudsen compressor in transitional flow. Journal of Vacuum Science & Technology A: Vacuum, Surfaces, and Films. 2002;20(1):214-24.
11.	Yen-Lin H. Thermal-Creep-Driven Flows in Knudsen Compressors and Related Nano/Microscale Gas Transport Channels. Microelectromechanical Systems, Journal of. 2008;17(4):984-97.
12.	Pharas K, McNamara S. Knudsen pump driven by a thermoelectric material. J Microelectromech Syst. 2010;20:125032.
13.	Vargo SE, Muntz EP, Shiflett GR, Tang WC. Knudsen compressor as a micro- and macroscale vacuum pump without moving parts or fluids. Journal of Vacuum Science & Technology A: Vacuum, Surfaces, and Films. 1999;17(4):2308-13.
14.	McNamara S, Gianchandani YB, editors. A micromachined Knudsen pump for on-chip vacuum. TRANSDUCERS, Solid-State Sensors, Actuators and Microsystems, 12th International Conference on, 2003; 2003 8-12 June 2003.
15.	Pharas K, McNamara S, Miles S. Thermal transpirational flow in the transitional flow regime. J Vac Sci Technol A Vac Surf Films Journal of Vacuum Science and Technology A: Vacuum, Surfaces and Films. 2012;30(5). English.

16.   Copic D, Brehob E, McNamara S, editors. Theoretical Efficiency of a Microfabricated Knudsen Pump. University/Government/Industry Micro/Nano Symposium, 2008 UGIM 2008 17th Biennial; 2008 13-16 July 2008.

17.   McNamara S, Gianchandani YB. On-Chip Vacuum Generated by a Micromachined Knudsen Pump. Microelectromechanical Systems, Journal of. 2005;14(4):741-6.

18.   Sharipov F. Rarefied gas flow through a long rectangular channel. Journal of Vacuum Science & Technology A: Vacuum, Surfaces, and Films. 1999;17(5):3062-6.

19.   Gupta NK, Gianchandani YB, editors. A high-flow Knudsen pump using a polymer membrane: Performance at and below atmospheric pressures. Micro Electro Mechanical Systems (MEMS), 2010 IEEE 23rd International Conference on; 2010 24-28 Jan. 2010.

20.   Pharas K, McNamara S, editors. Bi-directional gas pump driven by a thermoelectric material. Micro Electro Mechanical Systems (MEMS), 2010 IEEE 23rd International Conference on; 2010 24-28 Jan. 2010.

21.   Kreith F, Bohn MS, Manglik RM. Principles of heat transfer. Stamford, Conn.: Cengage Learning; 2011.

22.   Bell A, Pharas K, Ehringer WD, McNamara S, editors. Body temperature powered device for dermal wound drug delivery. Micro Electro Mechanical Systems (MEMS), 2012 IEEE 25th International Conference on; 2012 Jan. 29 2012-Feb. 2 2012.

23.   Bell A, Ehringer WD, McNamara S, editors. Wearable Infusion Pump Powered By Scavenged Body Heat. PowerMEMS; 2012 Dec 5-9; Atlanta, Georgia.

24.   Gupta NK, An S, Gianchandani YB, editors. A monolithic 48-stage Si-micromachined Knudsen pump for high compression ratios. Micro Electro Mechanical Systems (MEMS), 2012 IEEE 25th International Conference on; 2012 Jan. 29 2012-Feb. 2 2012.